Influence of deposition pressure on the adhesion of ZnO thin films deposited by cathodic vacuum arc deposition on polyimide foil substrates

Hu Changji[1]**, He Zhenhui**[1,3]**, Fu Weichun**[2] **and Zhong Qi**[2]

[1] State Key Laboratory of Optoelectronic Materials and Technologies, Center for Space Technology, and School of Physics and Engineering, Sun Yat-sen University, Guangzhou 510275, People's Republic of China
[2] China Academy of Spacecraft Technology, Beijing 100094, People's Republic of China

E-mail: stshzh@mail.sysu.edu.cn

Abstract
ZnO thin films, used as polymer protection layers against ultraviolet radiation and atomic oxygen for space application, were deposited on polyimide foil substrates using a cathodic vacuum arc deposition technique. A fragmentation test was employed to investigate the influence of deposition pressure on the adhesion of ZnO thin films. It was found that all the samples have good adhesive properties. Low deposition pressure is beneficial to the adhesion of ZnO films and polyimide substrates. Scanning electron microscopy was also employed to investigate the surface morphology of ZnO films that had suffered from large strain. No large areas of film detachment were found.

(Some figures in this article are in colour only in the electronic version)

1. Introduction

Polymeric materials represented by polyimide are widely used in space due to their unique properties, such as high strength-to-weight ratio, as well as a variety of mechanical, thermal, electrical and thermo-optical properties. However, in the low Earth orbit environment, they are subject to atomic oxygen (AO), ultraviolet (UV) radiation, ionizing radiation and extreme temperature variations, which shorten the lifetime of the material [1]. To protect polymers from these hazardous effects, many efforts have been made by introducing oxide coatings, such as SiO_2 and Al_2O_3, to the surface of polymers [2]. By comparison, ZnO thin film is better for this purpose in principle, since it possesses a wide band gap of 3.3 eV that absorbs UV radiation effectively [3]; and is resistant to high-energy radiation [4]. Among methods to prepare ZnO thin film on polymer substrates, such as pulse laser deposition (PLD), magnetron sputtering (MS) and cathodic vacuum arc

deposition (CVAD), CVAD has the advantages of a high ionization rate, high bombardment energy and high deposition rate. This makes it a promising method to deposit ZnO thin film on polyimide foil substrates [5]. Miyake *et al* have deposited Ga-doped ZnO films on a cyclo olefin polymer substrate by ion plating deposition (or CVAD) [6] and Herng *et al* have prepared copper-doped ZnO films on plastic (polycarbonate) substrates by the filtered cathodic vacuum arc technique [7]. These studies are focused on the structural, electrical or magnetic properties of the thin film. However, before these properties are exploited, adhesion to the substrate is an essential property that needs to be investigated [8]. Especially for oxide(or nitride)/polymer systems, due to the internal stress (including the thermal stress and the intrinsic stress), the large differences of thermal and mechanical properties between the polymer and the ceramics thin film may weaken the adhesion, and thus simultaneously weaken the performance of thin films [8]. Chaiwong *et al* have investigated the influence of thermal stress on the cracking of TiN films grown on polycarbonate

[3] Author to whom any correspondence should be addressed.

substrates by cathodic vacuum arc using the plasma immersion ion implantation and studied the adhesion of TiN by tensile testing using the ultimate shear strength to estimate the adhesion [9, 10]. Jacquet *et al* studied the adhesion of ZnO coatings deposited by RF MS on the surface of poly(ethylene naphthalate) films by a peeling test, and used the peeling energy to characterize the adhesion [11, 12]. Leterrier *et al* studied the adhesion of SiO_2 layer coated by physical vapour deposition on poly(ethylene terephthalate) films by a fragmentation test, and used the interfacial shear strength to evaluate the adhesion [13]. There are also some other methods to measure the adhesion of thin films on polymer substrates, such as the scratch test and the indentation test. Among these methods, the fragmentation test proved that it is applicable to a variety of thin brittle films on polymer substrates [14]. Since reports on the adhesion of oxide thin films prepared by CVAD to the polymer substrate are relatively few, in this paper, employing the fragmentation test, we studied mainly the adhesion of ZnO thin film to polyimide substrate, for the films prepared by CVAD at different deposition pressures.

2. Experimental

The CVAD system employed was described in [15]. A water-cooled Zn metal target (65 mm in diameter, 99.99% in purity) was used as a cathode. Supplied by Guangzhou Donghao Electrical Insulation Material Co. Ltd, the polyimide foil substrates, with a thickness of $50 \mu m$, were cleaned in isopropyl alcohol for 10 min in an ultrasonic bath, then dried with N_2 and finally mounted on a substrate holder. The distance between the cathode and the substrate holder was about 25 cm. After the chamber was evacuated to about $6.0 \times 10^{-6} Pa$, pure argon and oxygen gases were introduced in, with an Ar mass flow rate of 10 sccm and an O_2 mass flow rate of about 120 sccm. The deposition pressure was set to 0.9 Pa, 1.5 Pa and 2.8 Pa, respectively; the arc current was fixed to 50 A and the deposition time was 7 min for all the samples. The substrate was not intentionally heated during the deposition.

The residual (or internal) stress of the ZnO thin films can be obtained by the following equation [16]:

$$\sigma_{ZnO} = \frac{E_{ZnO}}{(1 + \nu_{ZnO})} \frac{\Delta 2\theta}{2 \tan \theta_0}, \qquad (1)$$

where σ_{ZnO} is the residual stress within the ZnO film, E_{ZnO} and ν_{ZnO} are the Young's modulus and the Poisson ratio of the ZnO film, respectively, $\theta_0 = 17.211$ is the Bragg angle under stress-free condition and $\Delta 2\theta$ is the difference between the measured 2θ and $2\theta_0$, which was obtained based on the x-ray diffraction $(0\,0\,2)$ peak of the ZnO films (see figure 2). Comparison of the diffraction peaks shows no difference between the measured 2θs before and after the fragmentation test described below.

A fragmentation test was carried out to evaluate the adhesion of the film. The tested films were not placed at the centre of the substrate holder and the distance between the cathode and the films was about 30 cm. The films were cut with a gauge 80 mm in length and 10 mm in width, then fixed on a home-made tensile device. The tensile device was placed under an Olympus BX51M optical microscope, and the
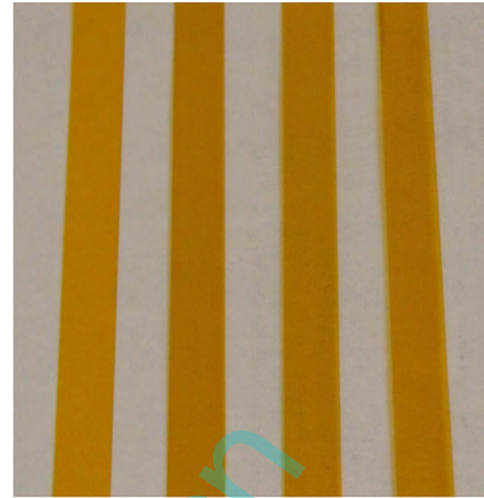
(a) bare (b) 0.9 Pa (c) 1.5 Pa (d) 2.8 Pa

Figure 1. Photograph of a bare polyimide film (a), and ZnO thin films deposited on polyimide substrates at the deposition pressure of (b) 0.9 Pa, (c) 1.5 Pa and (d) 2.8 Pa, respectively.
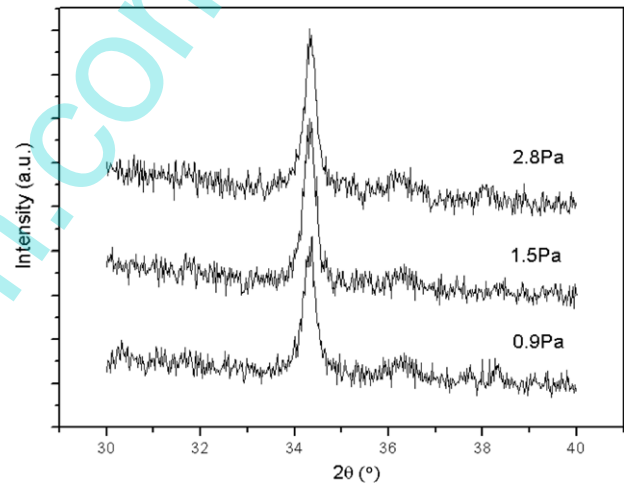
Figure 2. The x-ray diffraction patterns of the ZnO thin films deposited on polyimide foil substrates at the deposition pressures of 0.9, 1.5 and 2.8 Pa.

images of the cracks were taken by a CCD camera mounted onto the microscope. Post-analysis of crack morphology and composition was done using SEM/EDS on a thermal FE environment scanning electron microscope (QUANTA 400). The thicknesses of the tested films were determined by measuring the fragment thickness on the SEM image for the films after the fragmentation test, which agreed quite well with the crack depths measured by AFM (CSPM4000).

3. Results

All the surfaces of the deposited ZnO thin films are smooth, without any blistering, surface rippling and discoloration (see figure 1). The ZnO films are polycrystalline, belonging to the hexagonal wurtzite structure, with strong *c*-axis orientation (see figure 2). The internal stress of the ZnO thin films deposited at different pressures are listed in table 1. In

Table 1. Influence of deposition pressure on internal stress, practical adhesion and intrinsic adhesion of ZnO thin films deposited on polyimide substrates.

Deposition pressure (Pa)	2θ (°)	Internal stress (MPa)	Practical adhesion (MPa)	Intrinsic adhesion (MPa)
0.9	34.314 ± 0.009	-256.3 ± 30.2	81.3 ± 7.6	63.8 ± 6.9
1.5	34.339 ± 0.008	-197.0 ± 26.8	70.3 ± 3.3	51.5 ± 2.9
2.8	34.334 ± 0.010	-208.9 ± 33.6	67.8 ± 1.0	53.3 ± 1.2

general, the internal stress decreases as the deposition pressure increases.

A fragmentation test was performed to characterize the development of the crack pattern of each of the samples (see table 1). Only the results for the film deposited at 0.9 Pa are presented in figure 3. At 0.53% strain, only faint cracks are seen perpendicular to the stretching direction. With increasing strain, the number of such cracks increases, and the cracks become wider. With further stretching, cracks in parallel to the stretching direction (transverse cracks) start to appear at the strain of 5.50% and more appear at the strain of 9%. At 13.7% strain, the crack pattern becomes irregular due to the large deformation of the sample and a more transverse crack region is observed. The final crack inter-spacing (l_c) obtained will be used to calculate the interfacial strength later on by equation (3).

According to the Kelly–Tyson model [17], the interfacial shear strength τ can be calculated by

$$\tau = \frac{2d_f}{l_c}\sigma_{max}(l_c), \qquad (2)$$

where d_f is the thickness of the film, l_c the smallest fragment that can undergo failure, which is related to the crack density at saturation, CD_{sat}, defined by $l_c = (2/1.337CD_{sat})$, and $\sigma_{max}(l_c)$ is the cohesive strength of the film.

The cohesive strength of the film can be determined as follows [18]:

$$\sigma_{max}(l_c) = \beta\left(\frac{l_c}{l_0}\right)^{-1/\alpha}\Gamma\left(1 + \frac{1}{\alpha}\right), \qquad (3)$$

where α is the Weibull modulus, β is the Weibull scale factor and $l_0 = 1\,\mu m$. The Weibull parameters α and β are derived from a linear approximation of the initial part of the fragmentation diagram, where the average fragment size is reported as a function of applied strain in logarithmic coordinates. $\sigma_{max}(l_c)$ is a combination of the intrinsic cohesive strength $\sigma_{i,max}(l_c)$ and the partially relaxed internal stress σ_f:

$$\sigma_{max}(l_c) = \sigma_{i,max}(l_c) - \frac{1.337}{2}\sigma_f. \qquad (4)$$

The shear stress τ is the sum of the intrinsic shear stress τ_i and the internal shear stress τ_f.

$$\tau = \tau_i + \tau_f = \frac{2d_f}{l_c}\left(\sigma_{i,max}(l_c) - \frac{1.337}{2}\sigma_f\right). \qquad (5)$$

Here, the interfacial shear strength τ is used to characterize the practical adhesion. Assuming that after the large-strain stretch, the detached fragments are parts of the film, which
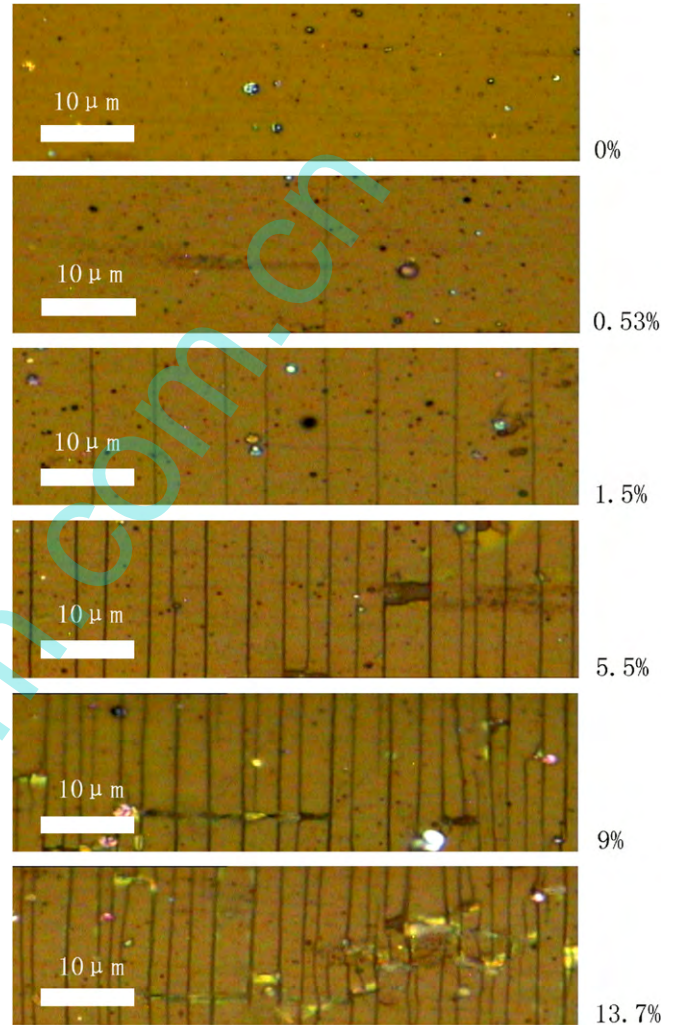
Figure 3. Development of the crack pattern as a function of strain for ZnO film deposited at 0.9 Pa.

are completely detached from the substrate at the interface, their thickness can be used to estimate the thickness of the film and used in equation (2) to calculate the interfacial shear strength. When the pressure increases from 0.9 to 2.8 Pa, τ decreases from about 81 to 68 MPa (see table 1). Taking the internal stress into account, we obtain the intrinsic interfacial shear strength that decreases from about 64 to 53 MPa. The interfacial strength of the sample having deposition pressure 0.9 Pa is comparable to that (84 MPa) of SiO$_2$/PET prepared by PECVD [18].

The SEM micrographs of the stretched ZnO samples clearly show detached fragments. These fragments are due to the compression caused by stretching the ZnO film deposited
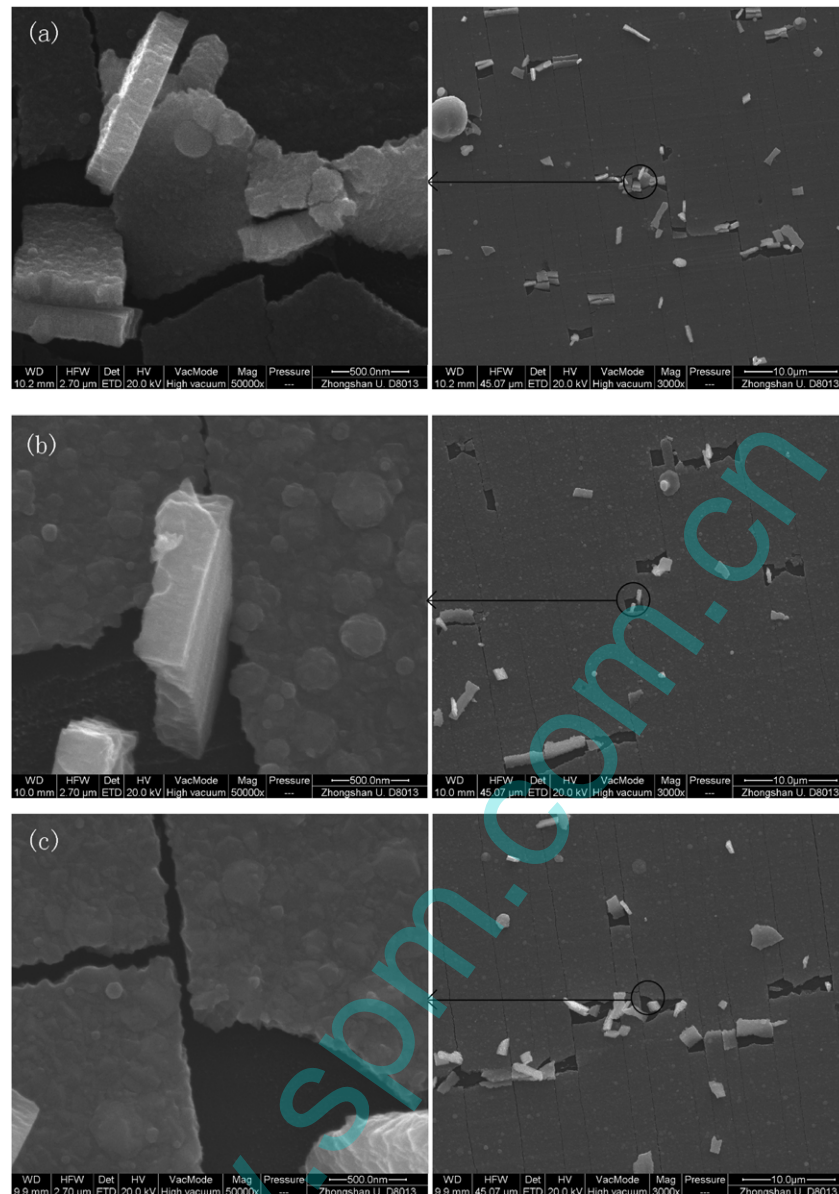
Figure 4. SEM micrographs of the ZnO samples, deposited at (*a*) 0.9 Pa; (*b*) 1.5 Pa and (*c*) 2.8 Pa, all after being stretched in the fragmentation test, with the ultimate tensile strain up to 13.7%.

on the polyimide substrate that has different Poisson's ratio (see figure 4). However, even at large strain (about 13.7%), no large areas of film detachment are found. Furthermore, the thicknesses of the fragments estimated from the SEM micrographs are about 190 nm, 300 nm and 330 nm for 0.9 Pa, 1.5 Pa and 2.8 Pa, respectively.

EDS mapping was carried out to investigate the Zn element distribution across the crack region. Only the results for the film deposited at 0.9 Pa are presented here in figure 5. The Zn content in the crack region is obviously lower than that of the film region, yet definitely higher than that on bare PI foil (table 2).

4. Discussion

Due to the binding force between the substrate and the films, when a load is applied to the substrate, it is transferred from the substrate to the film by means of shear force at the interface. When the shear force is lower than the cohesion force of the films, but larger than the fracture strength of the ZnO film, cracks perpendicular to the tensile axis appear. The intrinsic ZnO fracture strength, about 4 GPa for ZnO nanowires [20], is much higher than the interfacial strength obtained for the film. A closer view of the cracks (figure 4) shows that they develop along the boundaries of ZnO grains that compose the film. Thus, the fracture strength of the ZnO film represents the strength of the grain boundaries. Once the cracks appear, the interfacial stress is partially released until accumulated stress (shear force) causes more cracks at higher strain. At high strain, strain deformation is attributed to the substrate in the crack regions until the substrate failure occurs, since the ZnO film strengthens the substrate under the adhesive film. In this experiment, even upto the strain of the substrate failure, the cracked ZnO film (except for those fragments) still attaches
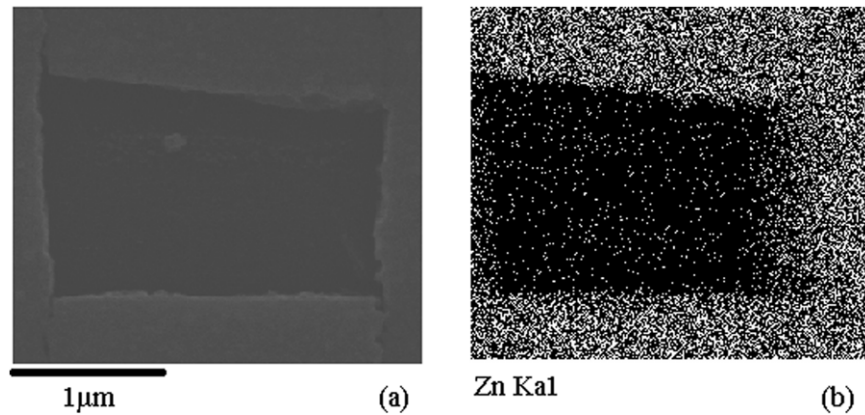
Figure 5. SEM image (*a*) and EDS mapping of Zn (*b*), of ZnO film deposited at 0.9 Pa, and had suffered from tensile strain of 13.7%.

Table 2. Atomic ratio of Zn/O in mapping region, crack region, film region and bare polyimide by EDS area analysis for which ZnO film (0.9 Pa) stretched to 13.7% strain.

	Atomic ratio (%)			
Element	Mapping region	Crack region	Film region	Bare PI
O K	79.4	93.0	67.8	99.5
Zn K	21.6	7.0	32.2	0.5

to the substrate. This is evidence of good adhesive properties of the films. Although the intrinsic interfacial shear strengths of films deposited at 1.5 Pa and 2.8 Pa are lower than that at 0.9 Pa, it is still comparable to the bulk shear yield strength of polyimide (about 60 MPa), estimated from the tensile data using equation (6):

$$\tau_y = \sigma_y/\sqrt{3}, \qquad (6)$$

where τ_y is the bulk shear yield strength of polyimide and σ_y is the tensile yield stress of the polymer film, obtained from tensile testing. This is an indication of good adhesive performance [13]. In the Kelly–Tyson model, the matrix (analogous to the polymer substrate) is assumed to be elastic up to the yield point and perfectly plastic beyond it [17]. No more stress can be transferred across the interface when the polymer substrate becomes completely plastic. Therefore, as long as the interfacial shear strength is higher than the polymer shear yield strength, the film will not detach from the substrate even if the polymer failure occurs. On the other hand, if the interfacial shear strength was lower than the polymer shear yield strength, the interface would have de-bonded and only frictional forces would have acted on the film.

In addition, the influences of deposition pressure on adhesion (see table 1) may be due to the effect of interfacial mixing. Since the energy of Zn ions in CVAD is relatively high (36 eV from the target [19]), sub-implantation caused by energetic ions is beneficial to the increase in the adhesion between the film and the substrate [21]. However, in the deposition process, the interaction between metallic plasma and neutral gas, such as elastic collisions and charge-exchange reaction, has a strong influence on the ion energy and ion flux distribution [22]. The energy of Zn ions (arriving at the substrate) decreases significantly with the deposition pressure, and the degree of interface mixing as well [23]. This accounts for the fact that the adhesion decreases as the deposition pressure increases.

Based on the EDS mapping of Zn distribution, compared with that of the bare polyimide substrate, the relatively high atomic ratio of Zn/O in the crack region suggests an indication of sub-implantation of Zn atoms or ions in the polymer substrate, supporting the existence of strong interfacial bonding between ZnO and the polyimide. For more details about the interfacial bonding, more electronic and structural information is called for of the interface between the film and the polyimide substrate.

5. Conclusion

In this study, the transparent ZnO thin films were deposited on polyimide foil substrates, by using CVAD, without actively heating the substrates. The samples exhibit good adhesive properties, especially for that deposited at the pressure of 0.9 Pa, with interfacial shear strength of about 81 MPa. Low deposition pressure is beneficial to the enhancement of adhesion between polyimide substrates and the ZnO films.

Acknowledgments

References

[1] Grossman E and Gouzman I 2003 Space environment effects on polymers in low earth orbit *Nucl. Instrum. Methods Phys. Res.* B **208** 48–57
[2] Kleiman J I, Iskanderova Z A, Pérez F J and Tennyson R C 1995 Protective coatings for LEO environments in spacecraft applications *Surf. Coat. Technol.* **76–77** 827–34

J. Phys. D: Appl. Phys. **42** (2009) 185303

H Changji *et al*

[3] Giancaterina S, Ben Amor S, Bachari E M, Baud G, Jacquet M and Perrinb C 2001 Elaboration and adhesion of zinc oxide coatings on poly-ether-ether-ketone films *Surf. Coat. Technol.* **138** 84–94

[4] Özgür Ü *et al* 2005 A comprehensive review of ZnO materials and devices *J. Appl. Phys.* **98** 041301

[5] Sanders D M and Anders A 2000 Review of cathodic arc deposition technology at the start of the new millennium *Surf. Coat. Technol.* **133–134** 78–90

[6] Miyake A, Yamada T, Makino H, Yamamoto N and Yamamoto T 2008 Effect of substrate temperature on structural, electrical and optical properties of Ga-doped ZnO films on cycro olefin polymer substrate by ion plating deposition *Thin Solid Films* **517** 1037–41

[7] Herng T S, Lau S P, Yu S F, Yang H Y, Teng K S and Chen J S 2007 Ferromagnetic copper-doped ZnO deposited on plastic substrates *J. Phys.: Condens. Matter* **19** 236214

[8] Ohring M 2006 *Materials Science of Thin Films: Deposition and Structure* (New York: Academic) pp 764–72

[9] Chaiwong C, McKenzie D R and Bilek M M M 2007 Cracking of titanium nitride films grown on polycarbonate *Surf. Coat. Technol.* **201** 5596–600

[10] Chaiwong C, McKenzie D R and Bilek M M M 2007 Study of adhesion of TiN grown on a polymer substrate *Surf. Coat. Technol.* **201** 6742–4

[11] Bachari E M, Ben Amor S, Baud G and Jacquet M 2001 Photoprotective zinc oxide coatings on polyethylene terephthalate films *Mater. Sci. Eng.* B **79** 165–74

[12] Guedri L, Ben Amor S, Gardette J L, Jacquet M and Rivaton A 2005 Lifetime improvement of poly(ethylene naphthalate) by ZnO adhesive coatings *Polym. Degrad. Stab.* **88** 199–205

[13] Howells D G, Henry B M, Leterrier Y, Månson J-A E, Madocks J and Assender H E 2008 Mechanical properties of SiO_x gas barrier coatings on polyester films *Surf. Coat. Technol.* **202** 3529–37

[14] Leterrier Y 2003 Durability of nanosized oxygen-barrier coatings on polymers *Prog. Mater. Sci.* **48** 1–55

[15] Zhu D, Zheng C, Liu Y, Chen D, He Z, Wen L, Cheung W Y and Wong S P 2006 Influence of bias voltage on morphology and structure of MgO thin films prepared by cathodic vacuum arc deposition *Surf. Coat. Technol.* **201** 2387–91

[16] Hsu Y-H, Lin J and Tang W C 2008 RF sputtered piezoelectric zinc oxide thin film for transducer applications *J. Mater. Sci.: Mater. Electron.* **19** 653–61

[17] Kelly A 1965 Tensile properties of fibre-reinforced metals: copper/tungsten and copper/molybdenum *J. Mech. Phys. Solids* **13** 329

[18] Rochat G, Leterrier Y, Fayet P and Månson J-A E 2003 Mechanical analysis of ultrathin oxide coatings on polymer substrates in situ in a scanning electron microscopy *Thin Solid Films* **437** 204–10

[19] Yushkov G Y, Anders A, Oks E M and Brown I G 2000 Ion velocities in vacuum arc plasma *J. Appl. Phys.* **88** 5618–22

[20] Hoffmann S, Östlund S, Michler J, Fan H J, Zacharias M, Christiansen S H and Ballif C 2007 Fracture strength and Young's modulus of ZnO nanowires *Nanotechnology* **18** 205503

[21] Monteiro O R 2001 Thin film synthesis by energetic condensation *Annu. Rev. Mater. Res.* **31** 111–37

[22] Minotti F O , Kelly H and Lepone A 2002 Two-dimensional fluid model for the inter-electrode region of a non-filtered vacuum arc *Plasma Sources Sci. Technol.* **11** 294–300

[23] Yang L, Zou J and Chen Z 1997 Ion energy measurements in vacuum arc deposition *IEEE Trans. Plasma Sci.* **25** 700–2